Solvability of the Viewing Graph Under the Affine Camera Model

Supplementary Material

In this document we include further analysis about viewing graph solvability under the affine camera model. More precisely, Sec. A reports further examples and theoretical analysis, Sec. B reviews basic notions on parallel rigidity, while Sec. C reports some considerations on the size of the matrices used by the various solvability/rigidity tests discussed in Sec. 6 (Experiments) of the main paper.

A. Additional Examples

First, we focus on the smallest solvable graph, which is the complete graph with $n = 3$ nodes, representing a triplet of cameras fully connected by three fundamental matrices (i.e., a "triangle", see Fig. 3a). This graph turns out to be affine solvable based on the outcome of our method (Algorithm 1), as already discussed in Sec. 4.2. However, it is also interesting to provide a formal proof of this fact.

Lemma 1. *Let $\mathcal{G}$ be the complete graph with three nodes: it is affine solvable.*

Proof. Let us denote the three affine cameras by O, P, Q and let us denote the three affine fundamental matrices by F_{PO}, F_{QO}, F_{QP}, where:

$$F_{QO} = \begin{bmatrix} 0 & 0 & a \\ 0 & 0 & b \\ c & d & e \end{bmatrix}, \quad F_{QP} = \begin{bmatrix} 0 & 0 & \bar{a} \\ 0 & 0 & \bar{b} \\ \bar{c} & \bar{d} & \bar{e} \end{bmatrix}. \tag{11}$$

Given the triplet of fundamental matrices, the task is to show that the cameras O, P, and Q compatible with them are unique. Without loss of generality, we can set:

$$O = \begin{bmatrix} 0 & 1 & 0 & 0 \\ 0 & 0 & 1 & 0 \\ 0 & 0 & 0 & 1 \end{bmatrix}, \quad P = \begin{bmatrix} n_{11} & n_{12} & m_{13} & u_1 \\ n_{21} & n_{22} & m_{23} & u_2 \\ 0 & 0 & 0 & 1 \end{bmatrix} \tag{12}$$

where the first row of P can be set arbitrarily, corresponding to fixing the affine frame, and the remaining elements can be estimated from F_{PO} in closed-form [19]. The task is then to show that camera Q can be determined *uniquely*. Let

$$Q = \begin{bmatrix} m_{11} & m_{12} & m_{13} & t_1 \\ m_{21} & m_{22} & m_{23} & t_2 \\ 0 & 0 & 0 & 1 \end{bmatrix}. \tag{13}$$

Using Prop. 1 for the pair $\{O, Q\}$, the linear system in (6) is then of the form:

$$\begin{cases} m_{11}a + m_{21}b = 0 \\ m_{12}a + m_{22}b = -c \\ m_{13}a + m_{23}b = -d \\ t_1 a + t_2 b = -e. \end{cases} \tag{14}$$

Concerning the pair $\{P, Q\}$, we get:

$$\begin{cases} m_{11}\bar{a} + m_{21}\bar{b} = -n_{11}\bar{c} - n_{21}\bar{d} \\ m_{12}\bar{a} + m_{22}\bar{b} = -n_{12}\bar{c} - n_{22}\bar{d} \\ m_{13}\bar{a} + m_{23}\bar{b} = -n_{13}\bar{c} - n_{23}\bar{d} \\ t_1\bar{a} + t_2\bar{b} = -u_1\bar{c} - u_2\bar{d} - \bar{e}. \end{cases} \tag{15}$$

From the systems in (14), and (15), we have in total 8 linear equations, for the 8 unknowns of camera Q. These equations are linearly independent, implying uniqueness of the camera Q, unless $\begin{bmatrix} a & b \end{bmatrix}^\mathsf{T} \simeq \begin{bmatrix} \bar{a} & \bar{b} \end{bmatrix}^\mathsf{T}$. The latter happens only when the triplet of cameras are collinear: this can easily be confirmed from the fact that the epipoles $e_{QO} \simeq \begin{bmatrix} -b & a & 1 \end{bmatrix}^\mathsf{T}$, and $e_{QP} \simeq \begin{bmatrix} -\bar{b} & \bar{a} & 1 \end{bmatrix}^\mathsf{T}$ would be coincident if $\begin{bmatrix} a & b \end{bmatrix}^\mathsf{T} \simeq \begin{bmatrix} \bar{a} & \bar{b} \end{bmatrix}^\mathsf{T}$, which implies collinearity of camera centers of O,P, and Q. See [19] for formulas of epipoles for affine cameras. Observe that collinearity is excluded by the genericity assumption, hence the considered viewing graph is affine solvable. □

As a second example, we provide a general graph topology that is not affine solvable, reported in Fig. 7. This graph was also studied in [24, 38] in the uncalibrated case.

Lemma 2. *Let $\mathcal{G}_1, \mathcal{G}_2, \mathcal{G}_3, \mathcal{G}_4$ be arbitrary affine solvable graphs, and let $\mathcal{G}$ be the graph of the form reported in Fig. 7: $\mathcal{G}$ is not affine solvable.*

Proof. The reasoning is similar to the proof of Prop. 3. Since $\mathcal{G}_1, \mathcal{G}_2, \mathcal{G}_3$ and $\mathcal{G}_4$ are affine solvable, it means that – within each sub-graph – the reconstruction of cameras is unique up to an affine transformation. Suppose that such affine transformation has been fixed in $\mathcal{G}_1$ (to set the global ambiguity) and let us denote the unknown affine transformation of the other sub-graphs by A_i for $i = 2, \ldots, 4$. In order to reconcile these transformations into a single one, we should write equations for each of the four common nodes

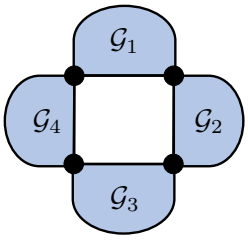

Figure 7. A viewing graph of this form is not affine solvable, where $\mathcal{G}_1, \mathcal{G}_2, \mathcal{G}_3$ and $\mathcal{G}_4$ are arbitrary affine solvable graphs.

highlighted in Fig. 7. For example, suppose the (known) camera in common between subgraphs $\mathcal{G}_1$ and $\mathcal{G}_2$ is denoted by P in $\mathcal{G}_1$ and by $\bar{P}$ in $\mathcal{G}_2$, hence we should solve $P = \bar{P}A_2$, which represents 8 equations in 12 unknowns (i.e., the entries of A_2). Doing this for the four common nodes gives rise to $8 \cdot 4 = 32$ equations in $12 \cdot 3 = 36$ unknowns: the resulting system is under-constrained, meaning that there is not enough information to have a single solution. In other terms, $\mathcal{G}$ is not affine solvable. □

B. Background on Parallel Rigidity

We now recall some basic notions about parallel rigidity, with specific focus on the 2D case, which is related to affine solvability. We refer the reader to [2] for more details.

Given a graph $\mathcal{G} = (\mathcal{V}, \mathcal{E})$, suppose that each node $i \in \mathcal{V}$ is associated with a point $\mathbf{x}_i \in \mathbb{R}^k$, and an edge $(i, j) \in \mathcal{E}$ is associated with the direction of the line joining $\mathbf{x}_i$ and $\mathbf{x}_j$:

$$\mathbf{u}_{ij} = \frac{\mathbf{x}_i - \mathbf{x}_j}{||\mathbf{x}_i - \mathbf{x}_j||}. \tag{16}$$

$\mathcal{G}$ is called *parallel rigid in k dimensions* if, for a given set of noiseless directions $\mathbf{u}_{ij}$ on the edges, then the node positions $\mathbf{x}_i$ can be *uniquely* recovered from the directions (up to translation and scale). The given directions are assumed compatible, i.e., at least a solution exists, and such solution is assumed to be generic (to exclude pathological cases like collinear points): the question is whether such solution is the only one (or not) with the given directions, in a similar way where we check for uniqueness of camera recovery from fundamental matrices in the context of solvability.

Parallel rigidity can be defined in any dimension k (what changes is the ambient space where one looks for possible solutions); if a graph is parallel rigid in k dimensions then it is so in $k + 1$ dimensions, but the converse is not true [2]. In the 2D case ($k = 2$), the concept can be visualized in Fig. 2 (main paper): the example at the bottom shows two configurations with the same directions (i.e., all edges are parallel in the geometric sense, like (1,2) with (1',2'), and similarly for the others), but they are not related by a *global* translation and scale, meaning that $\mathcal{G}$ is not parallel rigid.

2D parallel rigidity can be tested as follows: i) express parallelism constraints via the orthogonal projection as

$$\left(I - \frac{\mathbf{u}_{ij}\mathbf{u}_{ij}^{\mathsf{T}}}{||\mathbf{u}_{ij}||^2}\right)(\mathbf{x}_i - \mathbf{x}_j) = 0 \tag{17}$$

and collect equations of this form for all the edges into the so-called *bearing rigidity matrix* [2], with $\mathbf{u}_{ij}$ known and $\mathbf{x}_i$ unknown; ii) check if such a matrix has full rank, after fixing the global translation/scale ambiguity. In our experiments, we implement the probabilistic test based on the bearing rigidity matrix described above, where the input (noiseless) directions are obtained by sampling a random (hence generic with probability one) configuration of 2D points. We use the code provided by the authors of [30].

C. Size of Solvability/Ridigity Matrices

In this section we report some considerations about the complexity of the various solvability/rigidity tests evaluated experimentally in Sec. 6, that are summarized as follows:

- affine solvability (our method);
- 2D parallel rigidity [2];
- 3D parallel rigidity[2], which is equivalent to calibrated solvability [30], assuming that the essential matrix decomposition has been performed, so that the focus remains on camera positions only;
- uncalibrated solvability, which is approximated as finite solvability [6, 7], since checking solvability (i.e., uniqueness) would be intractable [3].

All the aforementioned methods require exactly the same operations, namely computing the rank of a proper matrix, which is equivalent to compute the Singular Value Decomposition and check if the smallest singular value is equal to zero. Note that there is no noise, as the starting point is a generic configuration of cameras, which in turn gives rise to noiseless fundamental matrices (see Steps 1-2 of Algorithm 1 for the affine case). A similar procedure applies to the other camera models and also to parallel rigidity [2]. To compute the rank of a matrix A, we used the default threshold as in Matlab's *rank* function: $r \times eps(||A||_2)$, where r is the number of rows of A, and $eps(x)$ is the distance from x to the next largest floating-point number.

Observe also that for all methods, the sparsity pattern of the involved matrices is similar, as each compatibility equation involves only one edge, i.e., two distinct nodes, but the other nodes are not involved. Hence, the complexity of the analyzed methods is in fact determined by the size of the respective matrices, which are reported in Tab. 4. Specifically, the number of equations corresponds to the number of rows, while the number of unknowns correspond to the number of columns. It should be noted, thought, that the reported numbers refer to the state of the art and they might not be the optimal number of equations/unknowns. For example, in the uncalibrated case, 12 parameters are used to

	#equations	#additional	#unknowns
2D Parallel rigid [2]	$2m$	3	$2n$
Affine Solvable (ours)	$4m$	12	$8n$
Uncalibrated Solvable [7]	$10m$	$n + 15$	$12n$
Calibrated Solvable [2]	$3m$	4	$3n$

Table 4. For different rigidity/solvability problems, the following information is reported: the number of equations associated to compatibility constraints between edge measures and node variables; the number of additional equations used to fix the global ambiguity; the number of unknowns. See references for details.

model cameras in [7] as 3×4 matrices (instead of 11 unknowns which would be the minimal case), and the scale ambiguity is managed via one extra equation per camera, resulting in n additional equations (which are added to the 15 equations representing the global projective ambiguity).

It is worth noting that affine solvability involves a smaller matrix than the uncalibrated case, in line with the fact that it is a simplified camera model. Another interesting observation is that the number of unknowns/equations is not the same for affine solvability and 2D rigidity: while this does not automatically disprove our conjecture on their equivalence, as a given solvability problem might be represented in many ways using different (but equivalent) formulations, at the same time we believe that this might represent a first step to prove (or disprove) our conjecture on the equivalence between affine solvability and 2D parallel rigidity. Future work will explore this direction.